IEEE Access
Multidisciplinary | Rapid Review | Open Access Journal

IEEE POWER & ENERGY SOCIETY SECTION

Received March 17, 2022, accepted April 30, 2022, date of publication May 4, 2022, date of current version May 11, 2022.

Digital Object Identifier 10.1109/ACCESS.2022.3172693

Robust Microgrid Scheduling Considering Unintentional Islanding Conditions

GUODONG LIU[1], (Senior Member, IEEE), THOMAS B. OLLIS[1], (Senior Member, IEEE), MAXIMILIANO F. FERRARI[1], (Member, IEEE), ADITYA SUNDARARAJAN[1], (Member, IEEE), AND KEVIN TOMSOVIC[2], (Fellow, IEEE)

[1]Electrical and Electronics System Research Division, Oak Ridge National Laboratory, Oak Ridge, TN 37831, USA
[2]Department of Electrical Engineering and Computer Science, The University of Tennessee, Knoxville, TN 37996, USA

Corresponding author: Guodong Liu (liug@ornl.gov)

This work was supported in part by the UT-Battelle, LLC with the U.S. Department of Energy under Contract DE-AC05-00OR22725; in part by the Engineering Research Center Program of the National Science Foundation and the Department of Energy through the Engineering Research Center Shared Facilities under NSF under Grant EEC-1041877; and in part by the Center for Ultra-wide-area Resilient Electric Energy Transmission Network (CURENT) Industry Partnership Program.

ABSTRACT This work presents a novel microgrid scheduling model considering the stochastic unintentional islanding conditions as well as forecast errors of both renewable generation and loads. By optimizing the dispatch of distributed energy resources (DERs), utility grid, and demand, the proposed model is targeted to minimize total operating cost of the microgrid, including start-up and shut-down cost of distributed generators (DGs), operation and maintenance (O&M) cost of DGs, cost of buying/selling power from/to utility grid, degradation cost of energy storage systems (ESSs) and cost associated with load shedding. To capture the stochastic unintentional islanding conditions and conventional forecast errors of renewable generation and loads, a two-stage adaptive robust optimization is proposed to optimize the objective function in the worst case scenario of the modeled uncertainties. The proposed optimization is solved with the column and constraint generation (C&CG) algorithm. The result obtained ensures robust microgrid operation in consideration of all possible realization of renewable generation, demand and unintentional islanding condition. The proposed model is validated with results of case studies on a microgrid consisting of various DGs and ESSs.

INDEX TERMS Robust scheduling, microgrids, uncertainty, unintentional islanding, column and constraint generation (C&CG).

NOMENCLATURE

The term (s) and (k) in the upper right position stands for scenario s and the k-th iteration, separately. A bold symbol stands for the corresponding vector.

A. INDICES

- i Index of dispatchable generators, running from 1 to N_G.
- d Index of loads, running from 1 to N_D.
- b Index of batteries, running from 1 to N_B.
- w Index of wind turbines, running from 1 to N_W.
- v Index of photovoltaic (PV), running from 1 to N_v.
- t Index of time intervals, running from 1 to N_T.
- s Index of scenarios, running from 1 to N_S.
- k, l Index of iterations.

B. VARIABLES

1) BINARY VARIABLES

- u_{it} 1 if unit i is scheduled on during period t and 0 otherwise.
- Z_t^{G} 1 if microgrid is grid-connected and 0 otherwise.

2) CONTINUOUS VARIABLES

- P_{it} Power output of unit i during period t.
- P_t^{PCC} Power at point of common coupling (PCC) during period t.
- P_{bt}^{C}, P_{bt}^{D} Charging/discharging power of battery b during period t.
- SOC_{bt} State of charge of battery b during period t.

The associate editor coordinating the review of this manuscript and approving it for publication was Guangya Yang.

P_{wt}^{W} Power output of wind turbine w during period t.
P_{vt}^{PV} Power output of PV panel v during period t.
P_{dt}^{L} Power consumption scheduled for load d during period t.
P_{dt}^{LS} Load shedding of load d during period t.
$\overline{\mu_{wt}}$, $\underline{\mu_{wt}}$ Auxiliary variables for forecast error of wind power P_{wt}^{W}.
$\overline{\mu_{vt}}$, $\underline{\mu_{vt}}$ Auxiliary variables for forecast error of PV power P_{vt}^{PV}.
$\overline{\mu_{dt}}$, $\underline{\mu_{dt}}$ Auxiliary variables for forecast error of load P_{dt}^{L}.

C. CONSTANTS

C_{bt} Degradation cost of battery b during period t.
C_{it}^{ON} Fixed operation and maintenance (O&M) cost of DG i during period t.
λ_{it} Variable O&M cost of DG i during period t.
λ_t^{PCC} Utility rate during period t.
$P_i^{\max}$, $P_i^{\min}$ Maximum/minimum output of DG i.
$P_t^{\mathrm{PCC,max}}$ Maximum PCC power during period t.
$\hat{P}_{wt}^{\mathrm{W}}$ Forecasted power output of wind turbine w during period t.
$\hat{P}_{vt}^{\mathrm{PV}}$ Forecasted power output of PV panel v during period t.
$\hat{P}_{dt}^{\mathrm{L}}$ Forecasted consumption of load d during period t.
$P_b^{\mathrm{C,max}}$, $P_b^{\mathrm{D,max}}$ Maximum charging/discharging power of battery b.
$SOC_{bt}^{\max}$, $SOC_{bt}^{\min}$ Maximum/minimum state of charge of battery b during period t.
η_b^{C}, η_b^{D} Battery charging/discharging efficiency factor.
δ_{wt}^{W}, $\delta_{vt}^{\mathrm{PV}}$, δ_{dt}^{L} Maximum deviations from the nominal forecast values $\hat{P}_{wt}^{\mathrm{W}}$, $\hat{P}_{vt}^{\mathrm{PV}}$ and $\hat{P}_{dt}^{\mathrm{L}}$.
Γ_t^{P} Robust control parameter of renewable generation and demand during period t.
γ_t^{P} Normalized robust control parameter of renewable generation and demand during period t.
Γ^{IS} Robust control parameter of unintentional islanding conditions.
γ^{IS} Normalized robust control parameter of unintentional islanding conditions.
$\triangle t$ Time duration of each period.
α_{dt} Maximum percentage of allowed shedding of demand d during period t.
π^s Probability of scenario s.

I. INTRODUCTION

A microgrid could be seen as a controllable local energy system consisting of various distributed generators (DGs), energy storage systems (ESSs) and energy consumers. Normally, a microgrid is connected to a utility grid through the Point of Common Coupling (PCC), but has the capability of operating independently [1]. When connected to the utility grid, a microgrid can not only import power from, or export power to the utility distribution network under different operational conditions, but also provide various kinds of ancillary services, e.g., frequency regulation, voltage support, virtual inertia, etc., to the utility grid [2]–[4]. For energy consumers, a microgrid can reduce carbon emission, improve energy efficiency, and serve low-cost and clean energy. In particular, through intentionally/unintentionally islanding from the utility grid, a microgrid is able to continue to supply power to its customers without any interruption when there is an outage on the utility gird, leading to improved energy reliability [5]. Because of these advantages, the study on microgrids has never been more popular [6].

Comparing with intentional islanding, i.e., a microgrid intentionally separates itself from the utility grid in case of foreseeable utility disturbances, unintentional islanding, i.e., a microgrid unintentionally separates itself from the utility grid driven by unforeseeable utility disturbances, is more important for reliability improvement since the vast majority of utility disturbances are unpredictable. Generally, a microgrid imports/exports power from/to the distribution grid in grid-connected mode, and this power is instantaneously forced to be zero when unintentional islanding happens. In this circumstance, the islanding process needs quick adjustment of the already committed DGs and ESSs, even load shedding as the last resort to mitigate the power imbalance caused by unintentional islanding and rebuild the balance between load and generation. To reduce or avoid load shedding and have the microgrid being prepared for possible unintentional islanding, certain amount of DGs should be committed and the ESSs should be charged to certain level. Nevertheless, there are two aspects of uncertainties associated with the unintentional islanding of microgrids. First, the occurrence time and duration of the unintentional islanding are uncertain. Second, the uncertainties in the forecasting of renewable generation and demand makes the problem more challenging. Therefore, development of new scheduling methods considering stochastic unintentional islanding conditions of microgrids and probabilistic characteristics of load and renewable generation is necessary for achieving the reliability benefit of microgrids.

So far, research work on microgrid scheduling considering the stochastic unintentional islanding conditions are still insufficient. In [7], an efficient joint implementation of Cuttle Fish Algorithm (CFA) and Crow Search Algorithm (CSA) method is proposed for optimum scheduling of microgrids with multi-period islanding restrictions. In [8], the probability that the microgrid is able to operate in islanded mode is formulated as a chance constraint. In [9], a probabilistic model to determine the spinning reserve requirement of microgrids is proposed. The uncertainty of contingency probability has been considered. In [10], the islanding capability

of a microgrid is modeled as a chance constraint and integrated into the original microgrid scheduling problem. The chance-constrained programming model is extended to include the reconfiguration of microgrids in [11]. In [12], a stochastic programming model is formulated for microgrid scheduling considering unscheduled islanding periods. The probability distribution of islanding duration is estimated and modeled by a scenario set. Nevertheless, the formulation of chance constraints needs probability distribution of renewable generation [8]–[11], and the generation of scenario set needs probability distribution function of unscheduled islanding periods [12]. In practice, information on both of them are very limited.

Unlike stochastic optimization, robust optimization only needs the upper and lower boundaries of the stochastic variables, neglecting their probability distributions and correlations. Thus, robust optimization has gained increasing popularity recently. In [13], a robust optimization model is proposed to quantify the reserve requirements of microgrids. Considering resiliency requirements, another robust optimization model is proposed for microgrid scheduling in [14]. However, both the occurrence time and duration of the unintentional islanding have been neglected. In [15], the multi-period islanding constraints are included in the microgrid scheduling model. The result guarantees microgrids could operate in islanded mode for certain hours specified by the microgrid operator. However, the occurrence time of the unintentional islanding has to be enumerated and the islanding duration has to be pre-set. The uncertainties of renewable generation and demand are considered in [16]. In [17], the uncertainties of renewable generation and grid-connection condition are included in the microgrid scheduling problem by formulating a two-stage robust optimization model. However, the uncertainty of load and the choice of load shedding have been ignored.

In this paper, given the stochastic unintentional islanding conditions of microgrids, a robust optimization model is proposed for optimal microgrid scheduling. The proposed model is guaranteed to serve local loads continuously through rapidly adjusting the output of committed DGs and ESSs whenever unintentional islanding happens. To capture the uncertainties in renewable generation, demand and the occurrence time and duration of the unintentional islanding, a two-stage adaptive robust optimization is proposed to optimize the objective function in the worst case scenario of the modeled uncertainties. The proposed optimization is solved with the column and constraint generation (C&CG) algorithm. The result obtained ensures robust microgrid operation in consideration of all possible realization of renewable generation, demand, and unintentional islanding conditions. The contributions of this work are twofold:

1) Considering the uncertainties of renewable generation, load and occurrence time and duration of the unintentional islanding, a two-stage robust optimization model is proposed. Using this model, microgrids are guaranteed to serve local loads continuously through rapidly adjusting the output of committed DGs and ESSs in case of unintentional islanding.
2) The optimal schedule obtained by the proposed robust optimization and stochastic optimization are tested through Monte Carlo simulation. The results demonstrate the robustness of the solution of proposed robust optimization.

This paper is structured as follows: both stochastic and robust models for microgrid scheduling considering the stochastic unintentional islanding conditions are presented in Section II. Section III describes the solution methodology. Section IV gives the numerical simulation results and analysis. The paper is concluded with major findings in Section V.

II. MATHEMATICAL FORMULATIONS

A. MICROGRID COMPONENTS

A microgrid is consisted of various distributed generators (DGs), ESSs and energy consumers. In practice, a microgrid central control (MCC) monitors the system running status and sends optimize dispatch orders to corresponding components. The DGs in a microgrid simply fall into two categories: dispatchable and undispatchable. Dispatchable DGs, e.g., small hydros, fuel cells, and microturbines, could be dispatched on demand at the request of MCC based on market needs or operator's preference. By contrast, undispatchable DGs, mainly referring to wind power and PV, are subject to uncertain nature of weather conditions, thus cannot be completely controlled by the MCC. In fact, wind power and PV power can only be forecasted with limited accuracy. For wind power, the hour-ahead forecast error could be made below 10%. However, the day-ahead forecast error is generally over 20% [18], [19]. As to PV power forecasting, the problem is getting more difficult due to random cloud coverage and changing ambient temperature, both of which affect the PV generation significantly [20], [21]. To mitigate the uncertainties of renewables, ESSs are normally installed on-site. Without loss of generality, both wind and PV power are assumed independent and bounded random variables in this work. The goal here is to guarantee continuous power supply of local demands through seamless islanding considering the uncertainties of renewables, load, and the occurrence time and duration of the unintentional islanding.

B. DETERMINISTIC OPTIMIZATION

In this subsection, the microgrid scheduling problem is modeled as a deterministic optimization model as in (1) - (9). The model is targeted to minimize total operating cost of the microgrid as shown in (1), including start-up, shut-down, fixed operation and maintenance (O&M), and variable O&M cost of DGs (as in the first line), cost of buying/selling power from/to utility grid (as in the second line), degradation cost of ESSs (as in the third line), and cost associated with load shedding (as in the fourth line).

$$\min \sum_{t=1}^{N_T} \sum_{i=1}^{N_G} \left[S_{it}^{\mathrm{U}} + S_{it}^{\mathrm{D}} + C_{it}^{\mathrm{ON}} u_{it} + \lambda_{it} P_{it} \right]$$

$$+\sum_{t=1}^{N_T}\lambda_t^{\mathrm{PCC}}P_t^{\mathrm{PCC}} +\sum_{t=1}^{N_T}\sum_{b=1}^{N_B}C_{bt}\left(P_{bt}^{\mathrm{C}}+P_{bt}^{\mathrm{D}}\right) +\sum_{t=1}^{N_T}\sum_{d=1}^{N_D}C_{dt}^{\mathrm{LS}}P_{dt}^{\mathrm{LS}} \quad (1)$$

$$s.t.\ P_i^{\min}u_{it}\le P_{it}\le P_i^{\max}u_{it}\quad \forall i,\ \forall t \quad (2)$$

$$0\le P_{bt}^{\mathrm{C}}\le P_b^{\mathrm{C,max}}\quad \forall b,\ \forall t \quad (3)$$

$$0\le P_{bt}^{\mathrm{D}}\le P_b^{\mathrm{D,max}}\quad \forall b,\ \forall t \quad (4)$$

$$SOC_{bt}=SOC_{b,t-1}+P_{bt}^{\mathrm{C}}\eta_b^{\mathrm{C}}\triangle t-P_{bt}^{\mathrm{D}}\frac{1}{\eta_b^{\mathrm{D}}}\triangle t\quad \forall b,\ \forall t \quad (5)$$

$$SOC_{bt}^{\min}\le SOC_{bt}\le SOC_{bt}^{\max}\quad \forall b,\ \forall t \quad (6)$$

$$\sum\nolimits_{i=1}^{N_G}P_{it}+\sum\nolimits_{w=1}^{N_W}P_{wt}^{\mathrm{W}}+\sum\nolimits_{v=1}^{N_{PV}}P_{vt}^{\mathrm{PV}}+P_t^{\mathrm{PCC}} +\sum\nolimits_{b=1}^{N_B}P_{bt}^{\mathrm{D}}-\sum\nolimits_{b=1}^{N_B}P_{bt}^{\mathrm{C}}=\sum\nolimits_{d=1}^{N_D}\left(P_{dt}^{\mathrm{L}}-P_{dt}^{\mathrm{LS}}\right)\quad \forall t \quad (7)$$

$$-Z_t^{\mathrm{G}}P_t^{\mathrm{PCC,max}}\le P_t^{\mathrm{PCC}}\le Z_t^{\mathrm{G}}P_t^{\mathrm{PCC,max}}\ \forall t \quad (8)$$

$$0\le P_{dt}^{\mathrm{LS}}\le \alpha_{dt}\%\hat{P}_{dt}^{\mathrm{L}}\quad \forall d,\ \forall t \quad (9)$$

The constraints of the microgrid scheduling problem includes power limits of DGs as in (2), charging and discharging power limits of ESSs as in (3) and (4), maximum and minimum state of charge (SOC) of ESSs as in (6), power limits at PCC as in (8), and maximum percentage of load shedding of each demand enforced by constraint (9). In addition, the SOC of an ESS is defined as a function its charging and discharging power as in (5). Due to the relatively small capacities of the DGs, the ramping rate limits of DGs have been neglected. Please refer to [22] for more detailed model of DGs. It should be noted that an optimal solution cannot have ESS charging and discharging at the same time due to the unnecessary losses caused by simultaneous charging and discharging. The total generation and load balance is guaranteed by equation (7). Note that Z_t^{G} in (8) is a binary indicator of grid-connection condition, which forces the PCC power to be zero if the microgrid is islanded.

The presented deterministic optimization model for microgrid scheduling is in mixed-integer linear form except S_{it}^{U} and S_{it}^{D}, which are the start-up and shut-down costs of DGs, separately. Nevertheless, both S_{it}^{U} and S_{it}^{D} could be easily reformulated into mixed-integer linear form. Please refer to [23] for details.

C. STOCHASTIC OPTIMIZATION

The deterministic optimization model presented in subsection II-B is extended into a two-stage stochastic optimization by considering various realization of renewable generation, load and grid-connection condition. In the first stage, the commitment status of DGs are determined before the realization of uncertainties and kept the same value for all scenarios. In the second stage, the uncertainties of renewable generation, load and grid-connection condition are realized into various scenarios. For each scenario, the PCC power, DGs and ESSs power, and load shedding are optimized correspondingly. The stochastic optimization model is presented as in (10) - (18).

$$\min \sum_{t=1}^{N_T}\sum_{i=1}^{N_G}\left(S_{it}^{\mathrm{U}}+S_{it}^{\mathrm{D}}+C_{it}^{\mathrm{ON}}u_{it}\right) +\sum_{s=1}^{N_s}\pi^s\left[\sum_{t=1}^{N_T}\sum_{i=1}^{N_G}\lambda_{it}P_{it}^s+\sum_{t=1}^{N_T}\lambda_t^{\mathrm{PCC}}P_t^{\mathrm{PCC,s}} +\sum_{t=1}^{N_T}\sum_{b=1}^{N_B}C_{bt}\left(P_{bt}^{\mathrm{C,s}}+P_{bt}^{\mathrm{D,s}}\right) +\sum_{t=1}^{N_T}\sum_{d=1}^{N_D}C_{dt}^{\mathrm{LS,s}}P_{dt}^{\mathrm{LS,s}}\right] \quad (10)$$

$$s.t.\ P_i^{\min}u_{it}\le P_{it}^s\le P_i^{\max}u_{it}\quad \forall i,\ \forall t,\ \forall s \quad (11)$$

$$0\le P_{bt}^{\mathrm{C,s}}\le P_b^{\mathrm{C,max}}\quad \forall b,\ \forall t,\ \forall s \quad (12)$$

$$0\le P_{bt}^{\mathrm{D,s}}\le P_b^{\mathrm{D,max}}\quad \forall b,\ \forall t,\ \forall s \quad (13)$$

$$SOC_{bt}^s=SOC_{b,t-1}^s+P_{bt}^{\mathrm{C,s}}\eta_b^{\mathrm{C}}\triangle t-P_{bt}^{\mathrm{D,s}}\frac{1}{\eta_b^{\mathrm{D}}}\triangle t \quad \forall b,\ \forall t,\ \forall s \quad (14)$$

$$SOC_{bt}^{\min}\le SOC_{bt}^s\le SOC_{bt}^{\max}\quad \forall b,\ \forall t,\ \forall s \quad (15)$$

$$\sum_{i=1}^{N_G}P_{it}^s+\sum_{w=1}^{N_W}P_{wt}^{\mathrm{W,s}}+\sum_{v=1}^{N_{PV}}P_{vt}^{\mathrm{PV,s}}+P_t^{\mathrm{PCC,s}} +\sum_{b=1}^{N_B}\left(P_{bt}^{\mathrm{D,s}}-P_{bt}^{\mathrm{C,s}}\right)=\sum_{d=1}^{N_D}\left(P_{dt}^{\mathrm{L,s}}-P_{dt}^{\mathrm{LS,s}}\right) \quad (16)$$

$$-Z_t^{\mathrm{G,s}}P_t^{\mathrm{PCC,max}}\le P_t^{\mathrm{PCC,s}}\le Z_t^{\mathrm{G,s}}P_t^{\mathrm{PCC,max}}\quad \forall t,\ \forall s \quad (17)$$

$$0\le P_{dt}^{\mathrm{LS,s}}\le \alpha_{dt}\%\hat{P}_{dt}^{\mathrm{L}}\quad \forall d,\ \forall t,\ \forall s \quad (18)$$

In the stochastic optimization model, the objective function is to minimize the expectation of the overall cost considering all possible scenarios. The constraints are basically the same as those of deterministic optimization model, but they have to be satisfied for each individual scenario. In specific, the commitment status of DGs are determined in the first stage and kept the same for all scenarios in the second stage. The second stage decisions, i.e., PCC power, output of DGs, charging/discharging power of ESSs and amount of load shedding, are changing along with the realization of renewable generation, load and grid-connection condition in each scenario. The stochastic model is reduced to deterministic model in the particular case when there is only one scenario.

P_{wt}^{W}, P_{vt}^{PV}, P_{dt}^{L} and Z_t^{G} are modeled as random variables with known probability distribution functions, based on which a set of scenarios is constructed through Monte Carlo simulation. Traditionally, load P_{dt}^{L} could be modeled as Gaussian distribution [24], [25]. Wind power P_{wt}^{W} is modeled as Gaussian distribution or Weibull distribution [26]. PV output P_{vt}^{PV} is modeled as Gaussian distribution or β

distribution [27]. The grid-connection condition Z_t^{G} is modeled as Bernoulli distribution [17]. An appropriate scenario set is critical to the efficiency of stochastic model. With more scenarios, the scenario set will be more precise. However, the computational intensity will be increased as well. To reduce the computational burden of the problem, backward scenario reduction has been commonly utilized to cut down the number of scenarios [28].

D. ROBUST OPTIMIZATION

The deterministic optimization model presented in subsection II-B is extended into a two-stage robust optimization by considering the variation of renewable generation, load and grid-connection condition. Unlike stochastic optimization, robust optimization doesn't require the probability distributions and correlations of the stochastic variables. Without loss of generality, wind power P_{wt}^{W}, PV power P_{vt}^{PV} and load P_{dt}^{L} are assumed independent, symmetric and continuous random variables as in (19). Meanwhile, the grid-connection condition Z_t^{G} is assumed binary random variable.

$$\begin{cases} P_{wt}^{\mathrm{W}} \in \left[\hat{P_{wt}^{\mathrm{W}}} - \delta_{wt}^{\mathrm{W}},\ \hat{P_{wt}^{\mathrm{W}}} + \delta_{wt}^{\mathrm{W}}\right], & \delta_{wt}^{\mathrm{W}} \geq 0 \\ P_{vt}^{\mathrm{PV}} \in \left[\hat{P_{vt}^{\mathrm{PV}}} - \delta_{vt}^{\mathrm{PV}},\ \hat{P_{vt}^{\mathrm{PV}}} + \delta_{vt}^{\mathrm{PV}}\right], & \delta_{vt}^{\mathrm{PV}} \geq 0 \\ P_{dt}^{\mathrm{L}} \in \left[\hat{P_{dt}^{\mathrm{L}}} - \delta_{dt}^{\mathrm{L}},\ \hat{P_{dt}^{\mathrm{L}}} + \delta_{dt}^{\mathrm{L}}\right], & \delta_{dt}^{L} \geq 0 \\ Z_t^{\mathrm{G}} \in \{0,\ 1\}, \end{cases} \tag{19}$$

The robust optimization model is formulated in "min-max-min" form, as presented in (20) - (23). Similar to stochastic optimization, the commitment status of DGs are determined in the first stage before the realization of uncertainties and kept the same value for all possible realization of uncertainties. The second stage decisions, i.e., the PCC power, DGs and ESSs power, and load shedding, are changing based on the worst realization of renewable generation, load and grid-connection condition. By searching and optimizing the worst scenario, the proposed robust optimization guarantees the feasibility and bottom line of the solution under all possible realization of uncertainties.

$$\begin{aligned} \min_{\mathbf{u}\in\mathbb{U}} & \sum_{t=1}^{N_T}\sum_{i=1}^{N_G} S_{it}^{\mathrm{U}} + S_{it}^{\mathrm{D}} + S_{it}^{\mathrm{ON}} \\ & + \max_{\mathbf{Z^G},\mathbf{P^W},\mathbf{P^{PV}},\mathbf{P^L}\in\mathbb{W}} \quad \min_{\mathbf{P},\mathbf{P^{PCC}},\mathbf{P^C},\mathbf{P^D},\mathbf{P^{LS}}\in\mathbb{X}} \\ & \left\{ \sum_{t=1}^{N_T}\sum_{i=1}^{N_G} \lambda_{it} P_{it} + \sum_{t=1}^{N_T} \lambda_t^{\mathrm{PCC}} P_t^{\mathrm{PCC}} \right. \\ & + + \sum_{t=1}^{N_T}\sum_{b=1}^{N_B} C_{bt}\left(P_{bt}^{\mathrm{C}} + P_{bt}^{\mathrm{D}}\right) \\ & \left. \sum_{t=1}^{N_T}\sum_{d=1}^{N_D} C_{dt}^{\mathrm{LS}} P_{dt}^{\mathrm{LS}} \right\} \end{aligned} \tag{20}$$

$$s.t.\ \mathbb{U} = \{\mathbf{u} :\ u_{it} \in \{0,\ 1\},\ \forall i,\ t;\} \tag{21}$$

$$\begin{aligned} \mathbb{W} = \Big\{ & \mathbf{P}^{\mathrm{W}} :\ P_{wt}^{\mathrm{W}} = \hat{P_{wt}^{\mathrm{W}}} - \underline{\mu_{wt}}\delta_{wt}^{\mathrm{W}} + \overline{\mu_{wt}}\delta_{wt}^{\mathrm{W}},\ \forall w,\ t \\ & \mathbf{P}^{\mathrm{PV}} :\ P_{vt}^{\mathrm{PV}} = \hat{P_{vt}^{\mathrm{PV}}} - \underline{\mu_{vt}}\delta_{vt}^{\mathrm{PV}} + \overline{\mu_{vt}}\delta_{vt}^{\mathrm{PV}},\ \forall v,\ t \\ & \mathbf{P}^{\mathrm{L}} :\ P_{dt}^{\mathrm{L}} = \hat{P_{dt}^{\mathrm{L}}} - \underline{\mu_{dt}}\delta_{dt}^{\mathrm{L}} + \overline{\mu_{dt}}\delta_{dt}^{\mathrm{L}},\ \forall d,\ t \\ & \underline{\mu_{wt}},\ \overline{\mu_{wt}},\ \underline{\mu_{vt}},\ \overline{\mu_{vt}},\ \underline{\mu_{dt}},\ \overline{\mu_{dt}} \in [0,\ 1],\ \forall w,\ v,\ d,\ t \\ & \sum_{w=1}^{N_W}\left(\underline{\mu_{wt}} + \overline{\mu_{wt}}\right) + \sum_{v=1}^{N_{PV}}\left(\underline{\mu_{vt}} + \overline{\mu_{vt}}\right) \\ & + \sum_{d=1}^{N_D}\left(\underline{\mu_{dt}} + \overline{\mu_{dt}}\right) \leq \Gamma_t^{\mathrm{P}},\ \forall t \\ & \mathbf{Z}^{\mathbf{G}} :\ \sum_{t=1}^{N_T}\left(1 - Z_t^{\mathrm{G}}\right) \leq \Gamma^{\mathrm{IS}},\ Z_t^{\mathrm{G}} \in \{0,\ 1\},\ \forall t \\ & Z_t^{\mathrm{G}} \leq 1 - (Z_{t-1}^{\mathrm{G}} - Z_t^{\mathrm{G}}), \\ & \forall t \in \left[1, \min\left(N_T, t + \Gamma^{\mathrm{IS}} - 1\right)\right]\Big\} \end{aligned} \tag{22}$$

$$\mathbb{X} = \left\{\mathbf{P}, \mathbf{P^{PCC}}, \mathbf{P^C}, \mathbf{P^D}, \mathbf{P^{LS}} : (2)\text{-}(9)\right\} \tag{23}$$

As to the constraints, $\mathbb{W}$ represents the modeled uncertainty. In $\mathbb{W}$, wind power, PV power and loads are all modeled as bounded intervals, where $\overline{\boldsymbol{\mu}}$ and $\underline{\boldsymbol{\mu}}$ are control variables for positive and negative forecast errors, separately. These forecast errors are aggregated and controlled through a robust control parameter $\Gamma_t^{\mathrm{P}} \in [0,\ N_W + N_{PV} + N_D]$. Given a Γ_t^{P}, the worst scenario happens when $\lfloor \Gamma_t^{\mathrm{P}} \rfloor$ of forecast error control variables ($\overline{\boldsymbol{\mu}}$ or $\underline{\boldsymbol{\mu}}$) equal 1, i.e., $\lfloor \Gamma_t^{\mathrm{P}} \rfloor$ of the uncertainties reach their upper bounds or lower bounds, and one of forecast error control variables ($\overline{\boldsymbol{\mu}}$ or $\underline{\boldsymbol{\mu}}$) equals $\left(\Gamma_t^{\mathrm{P}} - \lfloor \Gamma_t^{\mathrm{P}} \rfloor\right)$, i.e., one of the uncertainties varies up to $\left(\Gamma_t^{\mathrm{P}} - \lfloor \Gamma_t^{\mathrm{P}} \rfloor\right)\delta$. With $\Gamma_t^{\mathrm{P}} = 0$, no forecast errors are considered, i.e., the robust optimization model is reduced to deterministic model. With $\Gamma_t^{\mathrm{P}} = N_W + N_{PV} + N_D$, all uncertainties reach their upper bounds or lower bounds, i.e., the solution is most conservative. By setting different values for the robust control parameter Γ_t^{P}, the microgrid controller could get solutions with various degree of conservatism.

Similarly, Γ^{IS} is a robust control parameter for the unintentional islanding condition, which takes value in $[0,\ N_T]$. Given a Γ^{IS}, the solution is guaranteed to be feasible and bottom line for all possible scenarios in which up to Γ^{IS} time intervals are islanded. If $\Gamma^{\mathrm{IS}} = 0$, all Z_t^{G} will be 1, i.e., no unintentional islanding happens, while if $\Gamma^{\mathrm{IS}} = N_T$, the microgrid is islanded all the time, leading to the most conservative solution. The occurrence time and the duration of unintentional islanding is modeled through binary variable Z_t^{G}. The occurrence time of unintentional islanding is simply anytime from the first time interval to the last time interval. The duration of unintentional islanding is limited by the summation of $1 - Z_t^{\mathrm{G}}$. Without loss of generality, it is also assumed that the microgrid will be reconnected to the utility grid until the utility grid has been completely restored or the extreme event has passed. Thus, only one unintentional islanding incident happens during the scheduling horizon.

$\mathbb{U}$ represents the feasible region for the first stage decisions, i.e., DG commitment status, and $\mathbb{X}$ represents the feasible set for the second stage decisions, i.e., the power at PCC,

output of DGs and ESSs, and load shedding. In specific, constraints (2)-(9) of deterministic optimization model are included in $\mathbb{X}$. It should also be noted that the first stage decisions hold for all scenarios, but the second stage decisions are only for the identified worst scenario.

In reality, the microgrid energy management is performed in two steps. First, the proposed two-stage robust microgrid scheduling model is solved to determine the day-ahead commitment status of DGs without knowing the grid-connection condition. Then, in the second step, the grid-connection condition is revealed, the microgrid dispatches committed DGs, ESSs and responsive loads to meet the power balance in real-time. The two-stage robust optimization model is particularly designed to hedge against the uncertainty in grid-connection condition and guarantee the microgrid operating continuously when switching between grid-connected and islanded modes.

III. SOLUTION ALGORITHM

The proposed tri-level "min-max-min" model in (20)-(23) is presented in a compact matrix form as in (24) to (25).

$$\min_{\mathbf{u}\in\mathbb{U}} \left\{ A_0^{\mathrm{T}}\mathrm{u} + \max_{\mathbf{w}\in\mathbb{W}} \min_{\mathbf{x}\in\mathbb{X}(\mathbf{u},\mathbf{w})} B_0^{\mathrm{T}}\mathbf{w} + C_0^{\mathrm{T}}\mathbf{x} \right\} \tag{24}$$

$$\mathbb{X}(\mathbf{u},\mathbf{w}) = \left\{ \mathbf{x} : A_1^{\mathrm{T}}\mathrm{u} + B_1^{\mathrm{T}}\mathbf{w} + C_1^{\mathrm{T}}\mathbf{x} = \mathbf{q}_1, \right.$$
$$\left. A_2^{\mathrm{T}}\mathrm{u} + B_2^{\mathrm{T}}\mathbf{w} + C_2^{\mathrm{T}}\mathbf{x} \le \mathbf{q}_2; \right\} \tag{25}$$

Note that the three optimization levels are nested together. To solve this problem, the C&CG algorithm and Benders decomposition algorithm have been investigated in [29] and [30], separately. The C&CG algorithm is employed to solve the proposed robust optimization in this work due to proven fast convergence [29].

First of all, according to the Karush-Kuhn-Tucker (KKT) conditions, the innermost "min" optimization is reformulated as complementary constraints. Since this problem is linear, strong duality holds. The inner "max-min" problem becomes as follows:

$$\max_{\mathbf{w}\in\mathbb{W}} B_0^{\mathrm{T}}\mathbf{w} + C_0^{\mathrm{T}}\mathbf{x} \tag{26}$$

$$s.t.\ A_1^{\mathrm{T}}\mathbf{u}^k + B_1^{\mathrm{T}}\mathbf{w} + C_1^{\mathrm{T}}\mathbf{x} = \mathbf{q}_1 \tag{27}$$

$$C_0^{\mathrm{T}} + \beta^{\mathrm{T}}C_1 + \gamma^{\mathrm{T}}C_2 = 0 \tag{28}$$

$$0 \le \mathbf{q}_2 - A_2^{\mathrm{T}}\mathbf{u}^k - B_2^{\mathrm{T}}\mathbf{w} - C_2^{\mathrm{T}}\mathbf{x} \perp \gamma \ge 0 \tag{29}$$

where β is dual variable of equalities in (25), and γ is dual variable of inequalities. By Big-M method [31], the complementary constraint (29) could be equivalently transformed into (30) and (31) by introducing a binary variable δ and a large positive constant M.

$$0 \le \mathbf{q}_2 - A_2^{\mathrm{T}}\mathbf{u}^k - B_2^{\mathrm{T}}\mathbf{w} - C_2^{\mathrm{T}}\mathbf{x} \le \mathrm{M}\delta \tag{30}$$

$$0 \le \gamma \le \mathrm{M}(1-\delta) \tag{31}$$

Given DG commitment status $\mathbf{u}^k$ in iteration k, the "max" problem in (26) - (29) determines the worst scenario and calculates its objective value as $\mathcal{Q}(\mathbf{u}^k)$. Thus, $A_0^{\mathrm{T}}\mathbf{u}^{\mathrm{k}}+\mathcal{Q}(\mathbf{u}^k)$ is the objective value of the tri-level optimization problem with given $\mathbf{u}^k$. The true objective value of the tri-level optimization problem should be less than $A_0^{\mathrm{T}}\mathbf{u}^{\mathrm{k}}+\mathcal{Q}(\mathbf{u}^k)$ given the feasible region of $\mathbf{u}$. Therefore, the "max" problem in (26) - (29) generates an upper bound for the tri-level optimization problem. Note that the "max" problem is a subproblem with given $\mathbf{u}^k$.

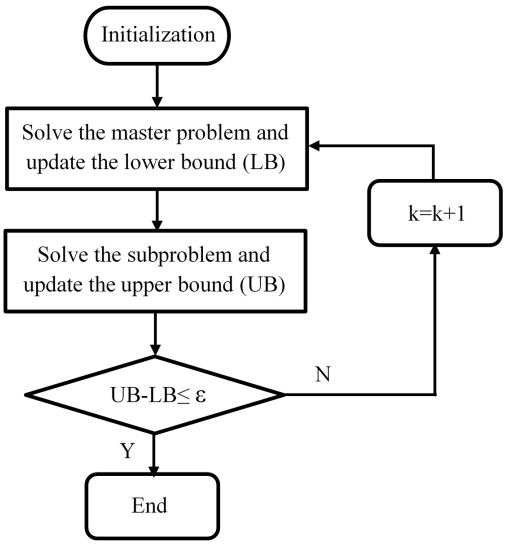

FIGURE 1. Solution process of the C&CG algorithm.

Based on the worst scenarios determined by the subproblem in (26) - (29), corresponding primal cuts are generated. By adding these primal cuts generated by the subproblem as constraints, the master problem in iteration k is updated as in (32)-(35).

$$\min_{\mathbf{u}\in\mathbb{U},\mathbf{x}^l} A_0^{\mathrm{T}}\mathrm{u} + \xi \tag{32}$$

$$s.t.\ \xi \ge B_0^{\mathrm{T}}\mathbf{w}^l + C_0^{\mathrm{T}}\mathbf{x}^l\ \forall l \le k \tag{33}$$

$$A_1^{\mathrm{T}}\mathrm{u} + B_1^{\mathrm{T}}\mathbf{w}^l + C_1^{\mathrm{T}}\mathbf{x}^l = \mathbf{q}_1\ \forall l \le k \tag{34}$$

$$A_2^{\mathrm{T}}\mathrm{u} + B_2^{\mathrm{T}}\mathbf{w}^l + C_2^{\mathrm{T}}\mathbf{x}^l \le \mathbf{q}_2\ \forall l \le k \tag{35}$$

where $\mathbf{w}^l$ is the worst scenario of uncertainties determined by subproblem (26) - (29) in the l-th iteration. $\mathbf{x}^l$ is the second stage decisions in this worst scenario. The master problem in (32) - (35) generates a lower bound for the tri-level optimization problem since the worst scenarios $\mathbf{w}^l$ are partial enumerations of the uncertainty region $\mathbb{W}$. In the C&CG algorithm, the master problem and subproblem are solved iteratively to narrow the gap between the upper and lower bounds until convergence. Fig. 1 presents the flow chart of the solution process.

It should be noted that the uncertainties of the parameters related to the cost have been neglected in the study. Considering these uncertainties, the term $C_0^{\mathrm{T}}\mathbf{x}$ in (26) will be bilinear. As a result, the subproblem becomes a bilinear problem. An outer approximation (OA) algorithm could be

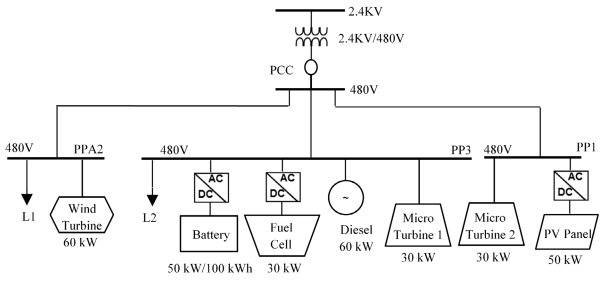

FIGURE 2. Modified ORNL DECC microgrid system.

TABLE 1. Dispatchable DG parameters.

DG Type	P^{min} (kW)	P^{max} (kW)	Start-up Cost ($)	Shut-down Cost ($)	Variable O&M Cost ($/kWh)	Fixed O&M Cost ($/h)
Diesel	20	60	3	1.5	0.5239	1
Microturbine 1	10	30	2	1	0.4507	1
Microturbine 2	10	30	1.5	0.75	0.3885	1
Fuel Cell	10	30	1	0.5	0.3385	1

TABLE 2. Battery parameters.

Battery Type	Power Capacity (kW)	Energy Capacity (kWh)	SOC^{max} (%)	SOC^{min} (%)
Lithium-ion	50	100	95	25
Degradation Cost ($/kWh)	Charging Efficiency (%)	Discharging Efficiency (%)	Initial SOC (%)	End SOC (%)
0.02	0.95	0.95	50	50

used to solve the bilinear programming [32], which linearizes the bilinear terms with respect to its values in the last iteration.

IV. CASE STUDIES

A. TEST SYSTEM DATA

The proposed model for microgrid scheduling considering the stochastic unintentional islanding conditions was demonstrated using a modified Oak Ridge National Laboratory (ORNL) Distributed Energy Control and Communication (DECC) microgrid test system. This system is consisted of multiple dispatchable DGs, undispatchable DGs (i.e., wind turbine and PV panel) and a battery, as shown in Fig. 2.

The parameters of dispatchable DGs are listed in Table 1. The parameters of the battery are listed in Table 2. Note that these DGs and the battery are the dispatchable resources in the microgrid.

A wind turbine with 60 kW rated capacity is installed in the microgrid. The wind power forecasted for the next 24-hour scheduling horizon are listed in Table 3. For the case of robust optimization, the forecast error of wind power is assumed $\pm$ 35%. The microgrid also has 50 kW PV panels installed. Similarly, the PV power forecasted for the next 24-hour scheduling horizon are listed in Table 4. For the case of robust optimization, the forecast error of PV power is also assumed $\pm$ 35%. Note that wind turbine and PV are the undispatchable resources in the microgrid.

TABLE 3. Forecasted wind power.

Hour	$\hat{P^W}$ (kW)	Hour	$\hat{P^W}$ (kW)	Hour	$\hat{P^W}$ (kW)
1	51.4829	9	21.7503	17	24.2732
2	38.3711	10	34.8202	18	26.2555
3	43.5590	11	27.1748	19	26.7732
4	40.7514	12	30.1965	20	26.2159
5	27.7421	13	23.5169	21	32.8428
6	30.1540	14	39.4794	22	36.0156
7	28.6452	15	35.738	23	37.2312
8	23.3767	16	18.0583	24	44.1215

TABLE 4. Forecasted PV power.

Hour	$\hat{P^{PV}}$ (kW)	Hour	$\hat{P^{PV}}$ (kW)	Hour	$\hat{P^{PV}}$ (kW)
1	0	9	5.2978	17	14.1823
2	0	10	11.6044	18	4.6705
3	0	11	36.6382	19	0.1836
4	0	12	42.6778	20	0
5	0	13	35.2199	21	0
6	0	14	35.4594	22	0
7	0.1617	15	34.8303	23	0
8	1.7726	16	23.6244	24	0

TABLE 5. Forecasted total load.

Hour	$\hat{P^L}$ (kW)	Hour	$\hat{P^L}$ (kW)	Hour	$\hat{P^L}$ (kW)
1	124.7103	9	186.3319	17	187.0655
2	123.9769	10	190.7334	18	185.5983
3	126.9111	11	195.8685	19	183.3975
4	124.7103	12	189.9998	20	187.0655
5	128.3783	13	189.9998	21	190.7334
6	135.4320	14	187.0655	22	181.9303
7	146.7180	15	192.2006	23	161.3898
8	178.2624	16	194.4014	24	134.9806

TABLE 6. Forecasted utility rates.

Hour	λ^{PCC} (ct/kWh)	Hour	λ^{PCC} (ct/kWh)	Hour	λ^{PCC} (ct/kWh)
1	8.65	9	12.0	17	16.42
2	8.11	10	9.19	18	9.83
3	8.25	11	12.3	19	8.63
4	8.10	12	20.7	20	8.87
5	8.14	13	26.82	21	8.35
6	8.13	14	27.35	22	16.44
7	8.34	15	13.81	23	16.19
8	9.35	16	17.31	24	8.87

The total load of the microgrid is forecasted as in Table 5. These forecasted values are equally divided into 2 loads. The maximum percentage of allowed shedding for both loads are set as 80%. The value of lost load (VOLL) is set as 2 $/kWh and 1.5 $/kWh, separately. For the case of robust optimization, the forecast errors of both loads are assumed $\pm$ 9%.

The forecasted hourly utility rates are listed in Table 6. For simplicity, the forecast errors of utility rates have been neglected. The maximum power at PCC is set as 200 kW.

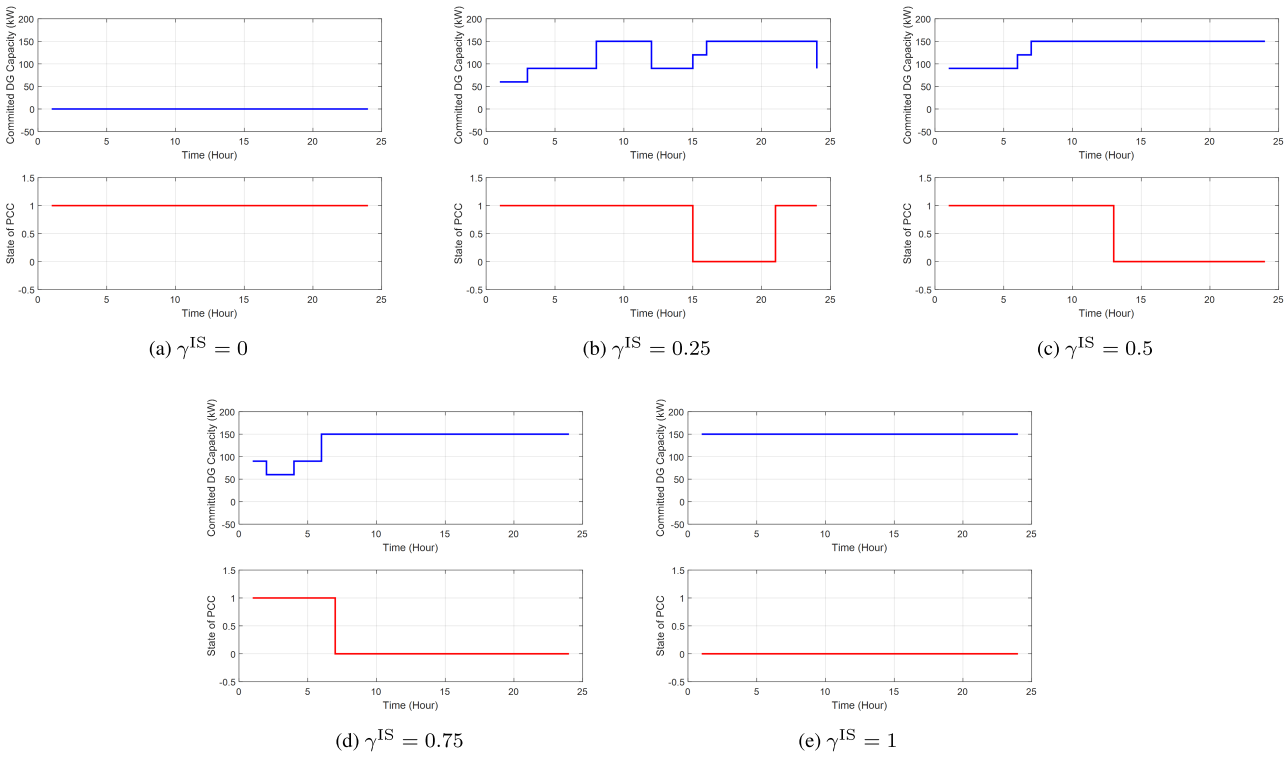

(a) $\gamma^{\mathrm{IS}} = 0$ (b) $\gamma^{\mathrm{IS}} = 0.25$ (c) $\gamma^{\mathrm{IS}} = 0.5$

(d) $\gamma^{\mathrm{IS}} = 0.75$ (e) $\gamma^{\mathrm{IS}} = 1$

FIGURE 3. Comparison of total capacity of committed DGs and worst scenario of unintentional islanding condition under various values of γ^{IS}.

The scheduling horizon is assumed one day, i.e., 24 hours, with hourly time intervals. The optimization model is programmed in MATLAB and solved by the mixed-integer linear programming (MILP) solver CPLEX 12.6 [33]. By setting the maximum allowed gap between the upper and lower bounds as 0.1, it generally takes less than 10 iterations for the C&CG algorithm to converge.

B. EFFECTS OF UNINTENTIONAL ISLANDING CONDITIONS

For simplicity, the robust control parameter for the unintentional islanding condition is normalized as $\gamma^{\mathrm{IS}} = \Gamma^{\mathrm{IS}}/N_T$. Thus, $\gamma^{\mathrm{IS}} = 0$ means no unintentional islanding is allowed and $\gamma^{\mathrm{IS}} = 1$ means the microgrid is islanded all the time. Similarly, we normalized the robust control parameter for renewable generation and load, as $\gamma^{P} = \Gamma_t^{\mathrm{P}} / (N_W + N_{PV} + N_D)$ and assume γ^{P} is same for all time intervals. Therefore, $\gamma^{P} = 0$ indicates no uncertainties of renewable generation and load are considered. On the contrary, $\gamma^{P} = 1$ means all uncertainties of renewable generation and load are considered, i.e., the solution is robust to all uncertainties.

Setting $\gamma^{P} = 0.5$, the results of proposed adaptive robust optimization with various robust control levels for the unintentional islanding condition are compared in this subsection. The total capacity of committed DGs and worst unintentional islanding condition under various values of γ^{IS} are compared in Fig. 3. As can be seen, no DGs are committed when $\gamma^{\mathrm{IS}} = 0$, due to the relatively low utility rate comparing with generation cost of DGs. As γ^{IS} increase, longer duration of unintentional islanding is taken into account. Thus, more committed DGs are needed to ensure the microgrid be prepared for all possible islanding events. When $\gamma^{\mathrm{IS}} = 1$, all DGs are committed.

The total operating cost and amount of load shedding under various values of γ^{IS} are compared in Fig. 4. With γ^{IS} increases, more DGs are committed. Meanwhile, more loads are served by DGs to mitigate the impact of lost PCC power in case of unintentional islanding. Thus, the total cost increases, i.e., the reliability of microgrids is improved at the cost of increased operating cost. If committed DGs and ESSs are not sufficient, certain loads are shed as the last resort. As shown in Fig. 4b, the amount of load shedding increases rapidly as the islanding condition is considered at first. However, the growth of load shedding slows down as γ^{IS} further increases.

C. CONVERGENCE OF C&CG ALGORITHM

The convergence process of C&CG algorithm with different robust levels is shown in this subsection. The lower and upper bounds calculated in each iteration are shown in Fig. 5a, when $\gamma^{\mathrm{IS}} = 0.25$ and $\gamma^{\mathrm{P}} = 0$, i.e., only uncertainties of unintentional islanding condition were considered. Considering the uncertainties of renewable generation and load, the lower and upper bounds calculated in each iteration are shown in Fig. 5b, when $\gamma^{\mathrm{IS}} = 0.25$ and $\gamma^{\mathrm{P}} = 0.5$. The algorithm converges after 9 iterations in both cases. Generally, the algorithm converges in less than 10 iterations.

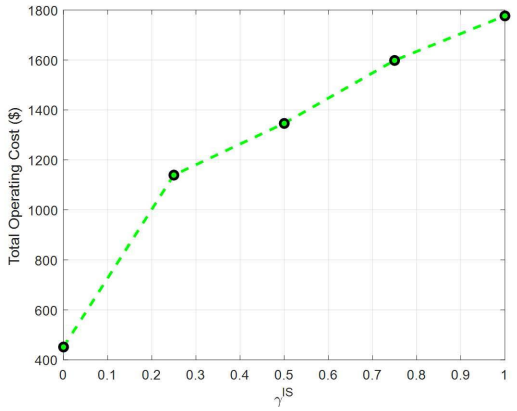

(a) Total operating cost

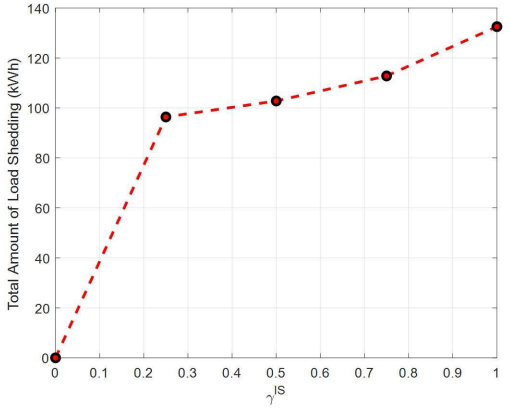

(b) Total load shedding

FIGURE 4. Comparison of total operating cost and amount of load shedding under various values of γ^{IS}.

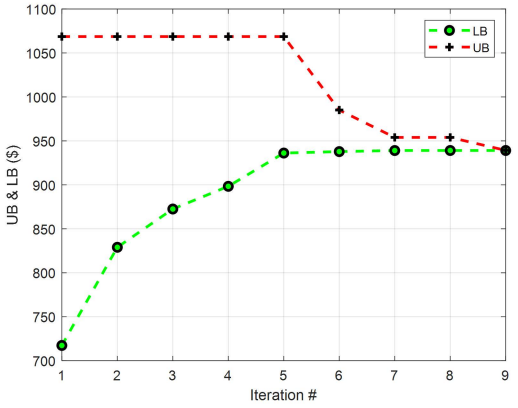

(a) $\gamma^{\mathrm{IS}} = 0.25, \gamma^{\mathrm{P}} = 0$

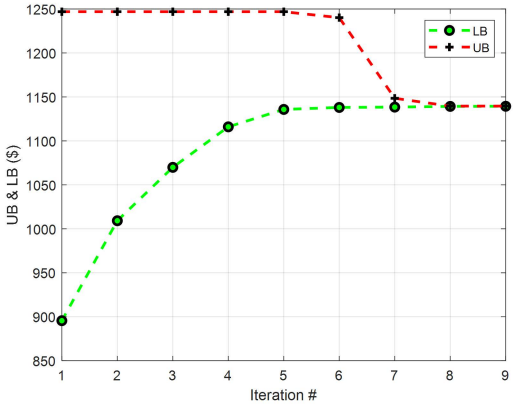

(b) $\gamma^{\mathrm{IS}} = 0.25, \gamma^{\mathrm{P}} = 0.5$

FIGURE 5. The convergence of the C&CG algorithm with various values of γ^{IS} and γ^{P}.

D. SOLUTIONS OF C&CG ALGORITHM

The robust optimal dispatch and the worst scenario of unintentional islanding condition when $\gamma^{\mathrm{IS}} = 0.25$ and $\gamma^{\mathrm{P}} = 0.5$ are shown in Fig. 6. As can be seen, in the worst scenario, the microgrid is islanded from hour 15 to hour 20, i.e., the PCC power is forced to be 0 during these hours. Meanwhile, the output power of DGs increases and the battery discharges. Also, load shedding is performed during certain hours. The PCC power, output power of DGs, battery SOC and load shedding decisions are shown in Fig. 6.

E. COMPARISON WITH STOCHASTIC OPTIMIZATION

In this subsection, the results of robust optimization and stochastic optimization are evaluated and compared under the same condition. For easy illustration, the uncertainties of renewable generation and load were ignored at first. The maximum islanding period is assumed 6 hours, i.e., $\Gamma^{\mathrm{IS}} = 6$ hours. For stochastic optimization, 100 scenarios are generated to model the unintentional islanding condition. For each scenario, the occurrence time of unintentional islanding are assumed uniform distribution along the scheduling horizon. Once the occurrence time is determined, the duration of

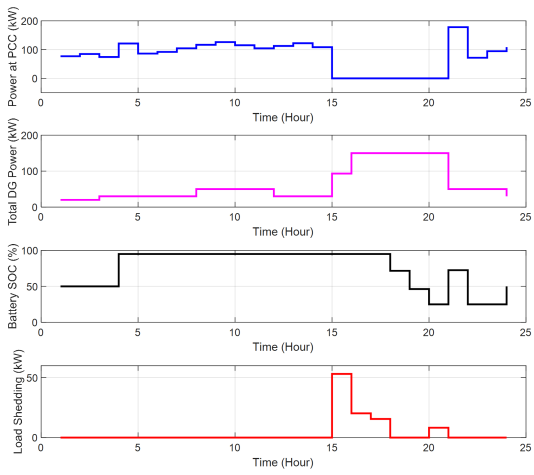

FIGURE 6. PCC power, output power of DGs, battery SOC and load shedding decisions under $\gamma^{IS} = 0.25$, $\gamma^{P} = 0.5$.

the unintentional islanding are assumed uniform distribution between 1 and Γ^{IS}. With these scenarios, the commitment status of DGs are determined by solving the stochastic optimization model. For robust optimization, we set $\gamma^{\mathrm{IS}} = \Gamma^{\mathrm{IS}}/N_T = 0.25$ and $\gamma^{\mathrm{P}} = 0$, and solve the robust optimization problem to determine the commitment status of DGs.

Next, a test set of 1000 scenarios is generated using the same distribution. For each test scenario, the first stage decisions, i.e., the commitment status of DGs, of both robust optimization and stochastic optimization are evaluated. The total operating cost and load shedding cost are collected. The minimum, maximum and average value of the total operating cost of both robust optimization and stochastic optimization are compared and shown in Fig. 7a. As can be seen, the stochastic optimization outperforms robust optimization in terms of average cost. However, the cost of stochastic optimization in the worst scenario is much higher than that of the robust optimization.

The minimum, maximum and average value of the load shedding cost of both robust optimization and stochastic optimization are compared and shown in Fig. 8b. As can be seen, the robust optimization outperforms stochastic optimization in terms of both average load shedding cost and the load shedding cost in the worst scenario.

It should be noted that load shedding cost is actually included in the total operating cost. From average point of view, the load shedding cost only takes a small percentage of the total operating cost. However, this percentage is increased significantly in the worst scenario, in which massive load shedding happens. In other words, the huge increase of total operating cost in the worst scenario is largely due to the significant increase of load shedding cost.

To consider the uncertainties of both renewable generation and load, wind power P^{W}_{wt}, PV power P^{PV}_{vt} and load P^{L}_{dt} are assumed independent, symmetric and bounded random variables as in (19). For robust optimization, we set $\gamma^{\mathrm{IS}} = 0.25$ and $\gamma^{\mathrm{P}} = 0.5$, and solve the robust optimization problem to determine the commitment status of DGs. For stochastic optimization, 100 scenarios are generated to model the unintentional islanding condition and uncertainties of renewable generation and load. For each scenario, the occurrence time and duration of unintentional islanding are generated using the same method. The loads are assumed normal distribution with mean $\hat{P^{\mathrm{L}}_{dt}}$ and standard deviation $\delta^{\mathrm{L}}_{dt}/3$. Thus, P^{L}_{dt} falls into the interval $\left[\hat{P^{\mathrm{L}}_{dt}} - \delta^{\mathrm{L}}_{dt},\ \hat{P^{\mathrm{L}}_{dt}} + \delta^{\mathrm{L}}_{dt}\right]$ with a probability of 99.7% based on the three-sigma rule of thumb (or 3σ rule). Similarly, the PV and wind power are also assumed normal distribution with mean $\hat{P^{\mathrm{PV}}_{vt}}$ and $\hat{P^{\mathrm{W}}_{vt}}$, and standard deviation $\delta^{\mathrm{PV}}_{vt}/3$ and $\delta^{\mathrm{W}}_{vt}/3$, separately. With these scenarios, the commitment status of DGs are determined by solving the stochastic optimization model.

Next, a test set of 1000 scenarios is generated using the same distribution. For each test scenario, the first stage decisions, i.e., the commitment status of DGs, of both robust optimization and stochastic optimization are evaluated.

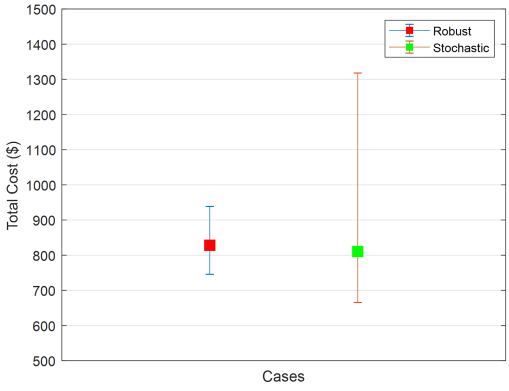

(a) Total operating cost

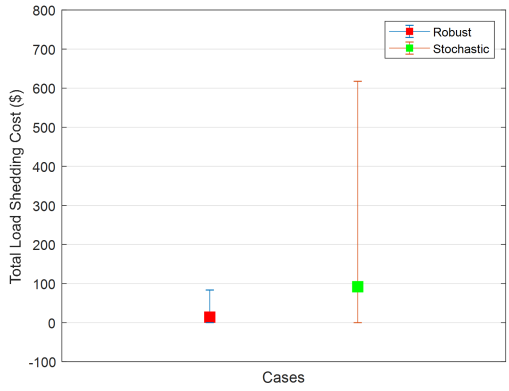

(b) Load shedding cost

FIGURE 7. Comparison of total operating cost and load shedding cost of stochastic and robust optimization with $\gamma^{\mathrm{IS}} = 0.25$ and $\gamma^{\mathrm{P}} = 0$.

The total operating cost and load shedding cost are collected. The minimum, maximum and average value of the total operating cost of both robust optimization and stochastic optimization are compared and shown in Fig. 8a. As can be seen, the average cost of robust optimization increases as we considered uncertainties of both renewable generation and load, while the average cost of stochastic optimization remains the same. In addition, the stochastic optimization outperforms robust optimization in terms of average cost. Nevertheless, the cost of stochastic optimization in the worst scenario is much higher than that of the robust optimization.

The minimum, maximum and average value of the load shedding cost of both robust optimization and stochastic optimization are compared and shown in Fig. 7b. As can be seen, the average load shedding cost of robust optimization increases as the more uncertainties are considered. Still, the proposed robust optimization outperforms stochastic optimization in terms of both average load shedding cost and the load shedding cost in the worst scenario.

It should be noted that the robust optimization tends to take a conservative action to handle the modeled uncertainties

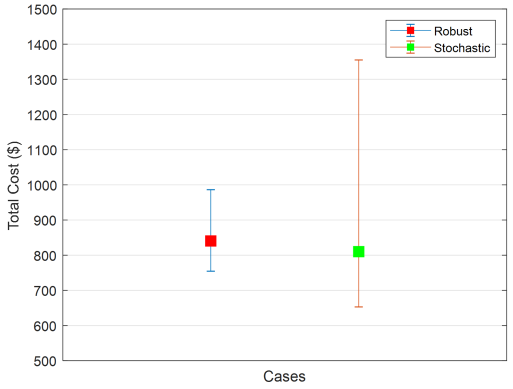

(a) Total operating cost

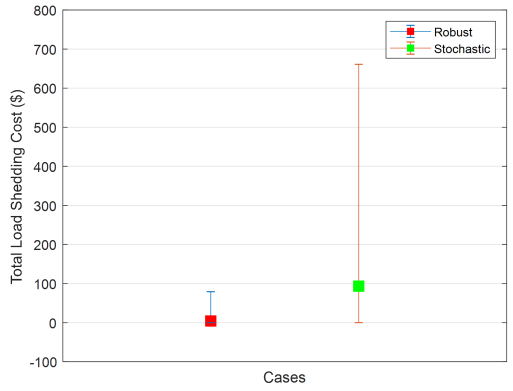

(b) Load shedding cost

FIGURE 8. Comparison of total operating cost and load shedding cost of stochastic and robust approach with $\gamma^{IS} = 0.25$ and $\gamma^{P} = 0.5$.

by turning on more DGs. Thus, stochastic optimization usually outperforms robust optimization in terms of average cost, as shown in Fig. 7a and Fig. 8a. For the same reason, robust optimization outperforms stochastic optimization in terms of average load shedding cost, as shown in Fig. 8b and Fig. 7b. In addition, stochastic optimization is subject to incur huge load shedding in high impact, low probability (HILP) scenarios. In contrast, robust optimization is designed to optimize the cost in the worst scenario, thus can significantly improve the system performance in HILP scenarios, i.e., reduce the load shedding in the worst scenario. In other words, robust optimization tends to sacrifice certain optimality for resilience.

Nevertheless, with properly chosen robust control parameters, the solution obtained by robust optimization can ensure both resilience and near-optimality. By the central limit theorem, when a large number (N) of independent random variables are aggregated, the volatility scales according to $O\left(\sqrt{N}\right)$. Therefore, a proper level of the normalized robust control parameter should be chosen close to $O\left(\sqrt{N}\right)/N$ [30]. An advanced approach, which reduces conservativeness by removing the ineffective parts of the uncertainty set, was recently proposed in [34].

V. CONCLUSION

Considering the stochastic unintentional islanding conditions, a novel microgrid scheduling model is proposed in this work. The proposed model is formulated as a two-stage adaptive robust optimization. The C&CG algorithm is employed to solve the formulated optimization. The solution ensures robust microgrid operation in consideration of all possible realization of renewable generation, demand and unintentional islanding condition. Numerical simulations on a modified microgrid test system verified the proposed model. In particular, the robustness of the solution of proposed optimization has been demonstrated by comparing with the results of stochastic optimization.

Future works include expanding islanding capability from simple power balance constraint to power flow constraint and dynamic stability constraint. In addition, distributed optimization algorithms, which could preserve privacy of customers and enable plug-and-play of microgrids, will be investigated.

ACKNOWLEDGMENT

The U.S. Government retains and the publisher, by accepting the article for publication, acknowledges that the U.S. Government retains a non-exclusive, paid-up, irrevocable, world-wide license to publish or reproduce the published form of this manuscript, or allow others to do so, for U.S. Government purposes. The Department of Energy will provide public access to these results of federally sponsored research in accordance with the DOE Public Access Plan (http://energy.gov/downloads/doe-public-access-plan).

REFERENCES

[1] A. Cagnano, E. D. Tuglie, and P. Mancarella, "Microgrids: Overview and guidelines for practical implementations and operation," *Appl. Energy*, vol. 258, Jan. 2020, Art. no. 114039.
[2] M. Z. Khan, C. Mu, S. Habib, W. Alhosaini, and E. M. Ahmed, "An enhanced distributed voltage regulation scheme for radial feeder in islanded microgrid," *Energies*, vol. 14, no. 19, p. 6092, Sep. 2021.
[3] B. Park, Y. Zhang, M. Olama, and T. Kuruganti, "Model-free control for frequency response support in microgrids utilizing wind turbines," *Electr. Power Syst. Res.*, vol. 194, May 2021, Art. no. 107080.
[4] R. Liu, S. Wang, G. Liu, S. Wen, J. Zhang, and Y. Ma, "An improved virtual inertia control strategy for low voltage AC microgrids with hybrid energy storage systems," *Energies*, vol. 15, no. 2, p. 442, Jan. 2022.
[5] Y. Wang, A. O. Rousis, and G. Strbac, "On microgrids and resilience: A comprehensive review on modeling and operational strategies," *Renew. Sustain. Energy Rev.*, vol. 134, Dec. 2020, Art. no. 110313.
[6] A. Hirsch, Y. Parag, and J. Guerrero, "Microgrids: A review of technologies, key drivers, and outstanding issues," *Renew. Sustain. Energy Rev.*, vol. 90, pp. 402–411, Jul. 2018.
[7] K. S. K. Kumari and R. S. R. Babu, "Optimal scheduling of a micro-grid with multi-period islanding constraints using hybrid CFCS technique," *Evol. Intell.*, vol. 15, no. 1, pp. 723–742, Mar. 2022.
[8] Y. Wu, G. J. Lim, and J. Shi, "Stability-constrained microgrid operation scheduling incorporating frequency control reserve," *IEEE Trans. Smart Grid*, vol. 11, no. 2, pp. 1007–1017, Mar. 2020.
[9] R. Li, M. Q. Wang, M. Yang, X. S. Han, Q. W. Wu, and W. L. Wang, "A distributionally robust model for reserve optimization considering contingency probability uncertainty," *Int. J. Electr. Power Energy Syst.*, vol. 134, Jan. 2022, Art. no. 107174.

[10] G. Liu, M. Starke, B. Xiao, X. Zhang, and K. Tonsovic, "Microgrid optimal scheduling with chance-constrained islanding capability," *Electr. Power Syst. Res.*, vol. 145, pp. 197–206, Apr. 2017.
[11] M. Hemmati, B. Mohammadi-Ivatloo, M. Abapour, and A. Anvari-Moghaddam, "Optimal chance-constrained scheduling of reconfigurable microgrids considering islanding operation constraints," *IEEE Syst. J.*, vol. 14, no. 4, pp. 5340–5349, Dec. 2020.
[12] H. Farzin, M. Fotuhi-Firuzabad, and M. Moeini-Aghtaie, "Stochastic energy management of microgrids during unscheduled islanding period," *IEEE Trans. Ind. Informat.*, vol. 13, no. 3, pp. 1079–1087, Jun. 2017.
[13] G. Liu, M. Starke, B. Xiao, and K. Tomsovic, "Robust optimisation-based microgrid scheduling with islanding constraints," *IET Gener., Transmiss. Distrib.*, vol. 11, no. 7, pp. 1820–1828, May 2017.
[14] G. Liu, T. B. Ollis, Y. Zhang, T. Jiang, and K. Tomsovic, "Robust microgrid scheduling with resiliency considerations," *IEEE Access*, vol. 8, pp. 153169–153182, 2020.
[15] A. Khodaei, "Microgrid optimal scheduling with multi-period islanding constraints," *IEEE Trans. Power Syst.*, vol. 29, no. 3, pp. 1383–1392, May 2014.
[16] A. Khodaei, "Resiliency-oriented microgrid optimal scheduling," *IEEE Trans. Smart Grid*, vol. 5, no. 4, pp. 1584–1591, Jul. 2014.
[17] Y. Guo and C. Zhao, "Islanding-aware robust energy management for microgrids," *IEEE Trans. Smart Grid*, vol. 9, no. 2, pp. 1301–1309, Mar. 2018.
[18] F. Shahid, A. Zameer, and M. Muneeb, "A novel genetic LSTM model for wind power forecast," *Energy*, vol. 223, May 2021, Art. no. 120069.
[19] E. Mora, J. Cifuentes, and G. Marulanda, "Short-term forecasting of wind energy: A comparison of deep learning frameworks," *Energies*, vol. 14, no. 23, p. 7943, Nov. 2021.
[20] R. Ahmed, V. Sreeram, Y. Mishra, and M. D. Arif, "A review and evaluation of the state-of-the-art in PV solar power forecasting: Techniques and optimization," *Renew. Sustain. Energy Rev.*, vol. 124, May 2020, Art. no. 109792.
[21] A. Sundararajan and B. Ollis, "Regression and generalized additive model to enhance the performance of photovoltaic power ensemble predictors," *IEEE Access*, vol. 9, pp. 111899–111914, 2021.
[22] H. Qiu, H. Long, W. Gu, and G. Pan, "Recourse-cost constrained robust optimization for microgrid dispatch with correlated uncertainties," *IEEE Trans. Ind. Electron.*, vol. 68, no. 3, pp. 2266–2278, Mar. 2021.
[23] M. Ortega-Vazquez, "Optimizing the spinning reserve requirements," in *School of Electrical & Electronics Engineering*. Manchester, U.K.: Univ. Manchester, 2006, pp. 1–219. [Online]. Available: http://www.eee.manchester.=ac.U.K./research/groups/eeps/publications/reportstheses/aoe/ortega-vazquez_PhD_2006.pdf
[24] B. Moradzadeh and K. Tomsovic, "Two-stage residential energy management considering network operational constraints," *IEEE Trans. Smart Grid*, vol. 4, no. 4, pp. 2339–2346, Dec. 2013.
[25] G. Liu and K. Tomsovic, "Robust unit commitment considering uncertain demand response," *Electr. Power Syst. Res.*, vol. 119, pp. 126–137, Feb. 2015.
[26] J. Morales, A. J. Conejo, and J. Perez-Ruiz, "Economic valuation of reserves in power systems with high penetration of wind power," *IEEE Trans. Power Syst.*, vol. 24, no. 2, pp. 900–910, May 2009.
[27] A. Fabbri, T. G. S. Roman, J. R. Abbad, and V. H. M. Quezada, "Assessment of the cost associated with wind generation prediction errors in a liberalized electricity market," *IEEE Trans. Power Syst.*, vol. 20, no. 3, pp. 1440–1446, Aug. 2005.
[28] J. Dupačová, N. Groewe-Kuska, and W. Roemisch, "Scenario reduction in stochastic programming: An approach using probability metrics," *Math. Program.*, vol. 95, no. 3, pp. 493–511, Jan. 2003.
[29] B. Zeng and L. Zhao, "Solving two-stage robust optimization problems using a column-and-constraint generation method," *Oper. Res. Lett.*, vol. 41, no. 5, pp. 457–461, Jun. 2013.
[30] D. Bertsimas, E. Litvinov, X. A. Sun, J. Zhao, and T. Zheng, "Adaptive robust optimization for the security constrained unit commitment problem," *IEEE Trans. Power Syst.*, vol. 28, no. 1, pp. 52–63, Feb. 2013.
[31] R. Jiang, J. Wang, and Y. Guan, "Robust unit commitment with wind power and pumped storage hydro," *IEEE Trans. Power Syst.*, vol. 27, no. 2, pp. 800–810, May 2012.
[32] R. Fletcher and S. Leyffer, "Solving mixed integer nonlinear programs by outer approximation," *Math. Program.*, vol. 66, nos. 1–3, pp. 327–349, Aug. 1994.
[33] (2016). *The ILOG CPLEX Website*. [Online]. Available: http://www-01.ibm.com/software/commerce/optimization/cplex-optimizer/index.html
[34] M. D. Filabadi and H. Mahmoudzadeh, "Effective budget of uncertainty for classes of robust optimization," *INFORMS J. Optim.*, to be published, doi: 10.1287/ijoo.2021.0069.

GUODONG LIU (Senior Member, IEEE) received the Ph.D. degree in electrical engineering from The University of Tennessee, Knoxville, TN, USA, in 2014. Since 2014, he has been a Research and Development Staff with the Electrical and Electronic System Research Division, Oak Ridge National Laboratory (ORNL), where he currently leads projects on microgrid operation and planning, renewable energy integration and active distribution network management. He is the major developer of CSEISMIC microgrid controller, Si-Grid, DECC microgrid, and RTDS-based microgrid testbed. He is the Principal Investigator of MADRA sponsored by the DOE Office of Electricity Delivery and Energy (DOE-OE). His research interests include power system operation and planning, power system reliability and security assessment, distributed energy resources, and microgrids.

THOMAS B. OLLIS (Senior Member, IEEE) received the B.S. and M.S. degrees in electrical engineering from The University of Tennessee, Knoxville. He began working at the Oak Ridge National Laboratory (ORNL), as a Student, in 2013, and joined the laboratory as a full-time Staff Member, in 2014. He worked as a Distribution System Operator in college and also in system planning for transmission and distribution systems at Duke Energy. He is currently a Research and Development Staff at the Grid Components and Controls Group, ORNL. His research interests include microgrids, battery energy storage, distribution market design, and renewable generation integration and control.

MAXIMILIANO F. FERRARI (Member, IEEE) received the B.S. degree in electrical engineering from the University of Javeriana, the M.S. degree in electrical engineering from the Polytechnic University of Valencia, and the B.S. degree in physics from the Allegheny College. He is currently pursuing the Ph.D. degree in energy sciences with The University of Tennessee, Knoxville. He is also a Research and Development Assistant Staff Member with the Grid Components and Controls Group, Oak Ridge National Laboratory. His research interests include microgrids, and controls for solar and wind energy systems and protection.

ADITYA SUNDARARAJAN (Member, IEEE) received the M.S. degree in computer engineering and the Ph.D. degree in electrical and computer engineering from Florida International University, Miami, in 2014 and 2019, respectively. Since 2020, he has been a Research and Development Associate Staff Member with the Grid Components and Controls Group, Oak Ridge National Laboratory. He has more than 50 publications in renowned journals and conference proceedings. His research interests include applied machine learning, artificial intelligence, and data analytics to address challenges in renewable integration, intelligent grids, systems development, and situation awareness. He received the Best Paper Award in 2017.

KEVIN TOMSOVIC (Fellow, IEEE) received the B.S. degree in electrical engineering from Michigan Technological University, Houghton, MI, USA, in 1982, and the M.S. and Ph.D. degrees in electrical engineering from the University of Washington, Seattle, WA, USA, in 1984 and 1987, respectively. He was on the faculty of Washington State University, Pullman, WA, from 1992 to 2008. He held the Advanced Technology for Electrical Energy Chair with Kumamoto University, Kumamoto, Japan, from 1999 to 2000, and was the NSF Program Director with the Electrical and Communications Systems Division of the Engineering Directorate, from 2004 to 2006. He is currently the CTI Professor with the Department of Electrical Engineering and Computer Science, The University of Tennessee, Knoxville, TN, USA, where he also directs the National Science Foundation (NSF)/Department of Energy (DOE) Research Center, for Ultra-Wide-Area Resilient Electric Energy Transmission Networks (CURENT), and worked as the Electrical Engineering and Computer Science Department Head, from 2008 to 2013.